Photoelectrocatalytic oxidation of methyl orange on TiO_2 nanotubular anode using a flow-cell

María José Martín de Vidales[1], Laura Mais[2], Cristina Sáez[1], Pablo Cañizares[1], Frank C. Walsh[3], Manuel A. Rodrigo[1], Christiane de Arruda Rodrigues[4], Carlos Ponce de León[3]*

[1]Department of Chemical Engineering, University of Castilla-La Mancha, Edificio Enrique Costa, Campus Universitario s/n. 13071 Ciudad Real, Spain

[2]Department of Mechanical, Chemical and Materials Engineering, University of Cagliari, Via Marengo 3, 09123 Cagliari, Italy

[3]Engineering Sciences, University of Southampton, Highfield, SO17 1BJ, Southampton, United Kingdom

[4]Federal University of São Paulo – Campus Diadema (UNIFESP – Campus Diadema), Departamento de Ciências Exatas e da Terra, Rua São Nicolau n◦210, 09913-030 Diadema, SP, Brazil

*Correspondence: Dr C. Ponce de Leon (E-mail: capla@soton.ac.uk), Engineering Sciences, University of Southampton, Highfield, SO17 1BJ, Southampton, United Kingdom

Abstract

Methyl orange from water was removed by photocatalytic anodic oxidation method using a titanium dioxide array surface. The coating was prepared by anodising a titanium plate using NH_4F as electrolyte followed by heat treatment to render a photocatalytic surface under UV light. SEM imaging showed that the array coating consisted of closely spaced 1 μm long, 0.1 μm internal diameter tubes perpendicular to the titanium plate. The aqueous solution of methyl orange was circulated through a rectangular channel flow cell containing the coated anode and the effect of electrolyte flow rate and applied potential on the oxidation rate and efficiency were evaluated. At higher mean linear flow rates, the efficiency of the oxidation process improved, indicating a mass transport controlled process. At more positive applied potentials the TiO_2 structure deteriorated resulted in lower oxidation efficiency.

Keywords: Flow cell, Methyl orange, Photoelectrocatalytic oxidation, TiO_2 nanotubes, Wastewater

1. Introduction

Stricter legislation for environmental protection continue to be implemented worldwide and methods to control the occurrence of pollutants in wastewaters are considered strategically important. Textiles industries can generate large amounts of wastewater with high concentrations dyes, affecting surface, ground and drinking waters. Such contaminants can be transformed into aromatic amines that conventional wastewater treatments are not able to degrade efficiently. These pollutants recalcitrant and pose a potential health risk to living organisms [1-3].

Received: February 10, 2015; revised: June 25, 2015; accepted: June 29, 2015

To be cited as: Chem. Eng. Technol. 10.1002/ceat.201500085

Link to final VoR: http://dx.doi.org/10.1002/ceat.201500085

Methyl orange, 4-[4-(dimethylamino)phenylazo] benzenesulfonic acid, $C_{14}H_{14}N_3NaO_3S$ is an intensely colored compound used in dyeing and printing textiles. It is also known commercially as C.I. acid orange 52, C.I. 13025, helianthine B, orange III, gold orange, and tropaeolin D. This azo dye is commonly used as an acid-base, its anionic form being yellow and its acidic form red.

New technologies able to degrade this complex pollutant efficiently and at low cost are needed and some developments have begun recently. These include advanced oxidation processes (AOPs) that aim to be clean and efficient, although many alternatives such as adsorption methods [4], flocculation [5] or biosorption [6] have also been proposed. Many of these technologies are separation processes and cannot completely remove the pollutants from the aqueous solution. Thus, AOPs are considered as a more efficient alternative for the complete oxidative degradation of organic compounds to carbon dioxide and water without the formation of residual compounds [7-17].

Photocatalytic processes have been studied to remove various dyes and high degradation percentages have been reported. Brillas and Martínez-Huitle, [18] compared the decontamination of wastewaters containing organic dyes by different electrochemical methods and highlight the high efficiency of the photocatalytic processes and its advantages when are carried out under solar energy. Specifically, Cardoso et al., [19] and Bansal et al., [20] studied the removal of aromatic amines by photoelectrocatalytic anodic oxidation using tubular titanium dioxide electrodes to degrade reactive red 35 dye. The authors discussed the reaction pathways and identified the reaction intermediates finding a 100 % decolorisation at pH 4. They reported that lower pH was not suitable due to the acid–base properties of TiO_2. Bessegato et al., [21] evaluated the performance of boron-doped TiO_2 nanotubes (B-TiO_2 NTs) prepared by electrochemical anodization and studying the degradation of Acid Yellow 1 dye. They pointed out that photoelectrocatalysis is an efficient and low cost method to remove hazardous organic compounds from water. Wu et al., [22] prepared TiO_2 nanotube electrodes to simultaneously produce hydrogen (i.e. water splitting) and degrade organic materials. They reported a photoconversion efficiency of 1.25 % at a photocurrent density of 1.52 mA cm^{-2} during the degradation of methylene blue while Wang et al. [23] reported the removal of methylene blue under ultraviolet and visible light and obtained a final degradation of about 95 %.

The above investigations show that photocatalytic oxidation can be effectively used to remove the colour caused by dyes found in wastewaters using TiO_2 nanotubes formed by anodizing Ti in aqueous electrolytes containing ammonium fluoride. The TiO_2 nanotubes formed on the anode surface typically had diameters between 20-90 nm and lengths of 200-500 nm depending on the anodising conditions. High nanotube areas led to large and more efficient photocurrents able to produce highly oxidizing hydroxyl radicals. Larger surface area improves the electron transfer at the anode surface [24, 25].

The voltage, electrolyte concentration, pH, time and heat treatment temperature are important parameters during the formation of photocatalytic TiO_2 nanotubes [26, 27]. The anodised nanotubes are amorphous above 300 ºC and should be submitted at heat treatment to crystallise [28]. According to Varghese et al. [29] the crystallization process in the anatase phase occurs close to 280°C. Near 430°C, the rutile phase emerges and the complete transformation to rutile occurs between 620–680 °C.

The majority of the studies reported in the literature use small glass cells and electrodes to study the degradation of the organics but there are fewer reports in an engineered flow cell containing anodised titanium anodes. In this paper, the goal is to study the removal of methyl orange (MO) as a model organic dye from wastewaters by photoelectrocatalytic oxidation at a TiO_2 nanotubular array coated anode in a flowing electrolyte cell to produce data aiding scale-up. The influence of the main oxidation parameters, such as the electrode potential and flow rate, are evaluated.

2. Materials and methods

2.1. Chemicals

The electrolyte used for anodising was prepared with ammonium fluoride (NH_4F) as received (Acros Organics) dissolved in ethylene glycol (Fisher Scientific) in 2 vol % of Milli-Q water. Synthetic solutions containing 0.25×10^{-3} mol L^{-1} methyl orange (> 99.0 % wt. purity, Acros Organics) in 0.1 mol L^{-1} sodium sulphate (Analytical Grade) were prepared with deionized water from a Millipore Milli-Q system (< 0.05 μS cm^{-1}).

2.2. Preparation of the TiO_2 nanotubular film

A titanium plate of 7.0 cm × 13.0 cm × 0.15 cm thick was mechanically polished and subjected to the following cleaning sequence: ultrasonication for 15 min in acetone, ethanol and Milli-Q water followed by drying the plate with nitrogen. Anodising was carried out with a nickel counter electrode of the same dimensions situated at 2 cm from the titanium plate. The electrolyte was 0.1 mol L^{-1} NH_4F and 2 % vol. Milli-Q water in ethylene glycol. The electrochemical treatment to generate the titanium nanotubes was a two-stage process beginning by increasing the cell potential from 0 V to 40 V at a linear rate of 2 V min^{-1} using a power supply (TTi-CPX400A, 60 V, 20 mA, Thurnby Thandar Instruments, UK) followed by holding the potential at 40 V for 100 minutes. After anodising, the electrode was washed with deionised water and dried in a nitrogen stream. The heat treatment was carried out in a Lenton Furnace and consisted in rising the temperature 23 ºC (room temperature) to 350 ºC at a rate of 2 ºC min^{-1}. The temperature was maintained constant for 30 min before increasing it to 450 ºC at 2 ºC min^{-1}. The temperature was maintained at 450 ºC for 150 minutes. Finally, the sample was left to cool down slowly to room temperature (23 ^{o}C).

2.3. Electrochemical cells

The electrochemical oxidation of MO was carried out in a single compartment electrochemical rectangular channel flow cell operating in the batch-recirculation mode [30]. The cell consisted of parallel transparent plates of 15.0 × 9.0 × 0.66 cm held together with a series of tie bolts and using silicone rubber gaskets between the plates to avoid leakage. One of the plates was made of quartz glass to allow the passage of the UV light while the others were acrylic. The titanium plate working electrode coated with TiO_2 nanotubes and the counter electrodes were slotted in between the plates and the interelectrode gap was 0.3 cm. The area of the electrodes exposed to the electrolyte was approximately 30 cm^2 and the working electrode had two 1 cm diameter holes at each corner to allow the entry and exit of the electrolyte into the flow channel as shown in Figure 1a. The counter electrode was a 0.15 thick titanium plate of area 7.0 cm × 13.0 cm. This plate had an empty space in the centre (4 cm × 9 cm) on which a 1.3 mm thick expanded titanium mesh, coated with

ruthenium mixed metal oxides, was spot welded. This electrode was attached to the quartz glass plate as shown in Figure 1a.

The reference electrode was Ag/AgCl (KCl, 3 mol L^{-1}) connected through a Luggin capillary positioned close to the working electrode. A computer controlled Autolab PGSTAT320-N potentiostat–galvanostat (Metrohm Autolab) was used for the electrochemical experiments. The ultraviolet lamp used was a CL1470-150-300 W Variable Xenon Power Supply Luxtel, positioned at approximate 9.0 cm from the working electrode. Figure 1b shows a schematic diagram of the electrochemical cell arrangement and the electrolyte circuit.

2.4. Experimental details

Cyclic voltammetry experiments were used to determine the electrode potentials at which the oxidation of methyl orange occurred and to find out the associated range of current densities under the ultraviolet-light irradiation (light intensity of 20.5 A). The laboratory scale electrolysis was carried out with 1000 cm^3 solution containing 0.25×10^{-3} mol L^{-1} of methyl orange in 0.1 mol L^{-1} Na_2SO_4 supporting electrolyte at a constant potential of 1.50 V or 1.75 V *vs*. Ag/AgCl. Following previous studies by Ma et al., [31] that indicate that the degradation of MO in wastewaters, by combined electrochemical processes, is more efficient at pH of approx. 3, the pH was adjusted to this value with H_2SO_4 and measured with an Acumet AP61 pH meter. Sodium sulphate was selected as an inert, supporting electrolyte since it has no effect on the electrolyte product. The simulated wastewater was circulated through the electrolytic cell by means of a magnetically driven centrifugal pump TE-3K-MD (March May) as shown in Figure 1b. The volumetric flow rate was controlled between 20 and 100 L h^{-1} (corresponding to a linear flow velocity past the electrode surface of 4.5-23.0 cm s^{-1}) and the experiments were carried out at 15 ºC by using a water bath as shown in Figure 1b.

The absorbance of 1 cm^3 aliquots taken at regular intervals of time during the electrolysis of the methyl orange solutions was measured by a UV/Visible spectroscopy (Scinco model Neosys-2000) at a maximum absorption wavelength of 500 nm. The absorbance was compared with those on a calibration plot previously constructed to determine the concentration of methyl orange. The morphology of TiO_2 nanotubes was imaged by a JEOL model JSM-6500F scanning electron microscope (SEM) equipped with energy dispersive X-ray spectroscopy SEM-EDS for elemental analysis. The TiO_2 phase composition was characterized by X-ray diffraction (XRD, Bruker D8 ADVANCE) using CuKα radiation.

3. Results and discussion

3.1. TiO_2 nanotubes

The TiO_2 nanotubes were synthesized by anodising in an NH_4F solution in ethylene glycol followed by heat treatment according to the procedure described in section 2.2 are shown in Figure 2. Figure 2a shows that the nanotubes are arranged at different levels within the titanium plate and that in general they are perpendicular to the electrode surface with a uniform distribution. Figure 2b is a close up of one of the gaps on the TiO_2 coating that reveals the diameter and depth of the nanotubes. The nanotubes are approx. 1 μm long with an outer diameter ca. 100 nm. These images show that the nanotubes have formed an optimal size distribution suitable for the oxidation of organic pollutants by photoelectrocatalysis [25].

The nanotubes produced by anodising are amorphous and were annealed to transform them into into crystalline phase TiO_2 nanotubes. Figure 3 shows an X-ray diffractogram of the TiO_2 nanotubular layer before and after the heat treatment, indicating the presence of anatase and rutile phases after the treatment at 450 °C. The relative intensity of the anatase peak is higher than that of the rutile peak after heat treatment, indicating that the TiO_2 nanotubular layer had acquired photocatalytic properties.

3.2. Effect of UV irradiation

Voltammetry curves in the absence and in the presence of 0.25×10^{-3} mol L^{-1} methyl orange in 0.1 mol L^{-1} Na_2SO_4 in the presence and the absence of UV light were obtained at a potential sweep rate of 0.01 V s^{-1}. Figure 4 shows these curves in the potential range between -0.25 and 1.75 V *vs*. Ag/AgCl. Curve a) represents an experiment carried out in the absence of MO at a UV lamp current of 20.5 A. The observed current density (0.9 mA cm^{-2}) in the voltammogram corresponds to the photocatalytic current generated by the TiO_2 nanotubes on the anode. Curve b) is the voltammogram in the presence of MO at the same UV radiation and current and curves c) and d) show that the photocurrent is negligible in the absence of UV radiation which suggests that the TiO_2 nanotubes alone are not catalytic towards the oxidation of MO.

When the UV radiation was present the magnitude of the current depended on the presence of methyl orange. The light received on the anodic surface is less when the solution contains MO as the dye partially blocks the UV light passing through the mesh electrode towards the anode. Another possibility for the decrease in the presence of the organic molecule could be due to some of the hydroxide radicals •OH intermediates oxidize the organic molecule inhibiting oxygen formation [32]. According to the voltammetry curve obtained with MO and in the presence of UV radiation (curve b), the removal of methyl orange via the photoelectrocatalytic oxidation can be carried out at constant potential electrolysis between the values of 0.25 and 1.75 V *vs*. Ag/AgCl. Higher positive potential values could destroy the structure and conductivity of titanium dioxide nanotubes as seen by Roy et al., [33].

3.3. Oxidation of MO; the influence of flow rate

Solutions containing 0.25×10^{-3} mol L^{-1} MO at pH 3 in 0.1 mol L^{-1} Na_2SO_4 as a supporting electrolyte were electrolysed at potential of 1.5 V *vs*. Ag/AgCl in order to remove the MO photoelectrocatalytically. Three electrolyte flow rates were evaluated using the UV lamp at an intensity of 20.5 A. Figure 5 shows the normalised concentration decay of methyl orange versus the electrical charge at three different flow rates: 20, 60 and 100 L h^{-1} (4.5, 6.3 and 23.0 cm s^{-1}). The curves show that the discoloration is faster as the flow rate increases. At 20 L h^{-1} (4.5 cm s^{-1}) the discoloration of methyl orange at a volumetric charge of 0.038 A h L^{-1} reached approximately 20 % whereas at higher flow rate of 100 L h^{-1} (23.0 cm s^{-1}) the discoloration was 55 %. Thus, the oxidation percentage achieved in this study is higher than for photolysis, photocatalytic or electrocatalytic processes, according to the studies reported by Zhou et al., [34] and Zheng and Lee, [35] using similar anodic materials.

There is a direct relationship between the electrolyte flow rate and the process efficiency; at 60 L h^{-1} (6.3 cm s^{-1}) and 100 L h^{-1} (23.0 cm s^{-1}), the oxidation of the organic compound is achieved with low values of electric charge and is relatively fast up to around 50 % oxidation. The fast discolouration observed a 100 L h^{-1} (23.0 cm s^{-1}) is due to the rapid removal of the

oxidation products that leaves the surface sites available. However, at a flow rate of 20 L h^{-1} (4.5 cm s^{-1}) the process efficiency is low due to the fact that the oxidation products are not removed faster and the start of the discolouration is slow down by the products being longer near the electrode surface, blocking the photocatalytic sites.

Figure 5 shows that the oxidation is mass transfer controlled however, the logarithm of the concentration decay *vs*. time (not shown) indicates that the oxidation rate at the start of the electrolysis is fast but slows down after certain time due to organic intermediates competing with methyl orange for the hydroxyl radicals. The formation of hydroxyl ions is electron transfer controlled at low applied charge (0.0015, 0.0025 and 0.005 A h L^{-1} for 20, 60 and 100 L h^{-1}, respectively). This indicates that the efficiency increases with the flow rate. At higher values of applied electric charge the discolouration profile follows similar linear decay trend *vs*. time in the three experiments but is slower [36].

3.4. Oxidation of MO; influence of the electrode potential

In order to study the influence of the applied electrode potential during the photoelectrocatalytic oxidation of MO, an additional experiment was carried out by increasing the applied electrode potential at 1.75 V *vs.* Ag/AgCl in a solution of 0.25×10^{-3} mol L^{-1} of MO in 0.1 mol L^{-1} Na_2SO_4 as supporting electrolyte at a flow rate of 100 L h^{-1}. Figure 6 shows the normalised concentration decay of MO at this electrode potential in comparison with the results when the electrode potential was 1.5 V *vs.* Ag/AgCl at the same flow rate. As it can be observed from the Figure 6, at a potential of 1.5 V *vs.* Ag/AgCl the oxidation of MO by photocatalytic oxidation seems to be more efficient and use lower electric charge for the same level of discolouration than when the discolouration was carried out at 1.75 V *vs*. Ag/AgCl. This was not the expected result; it might be expected that higher potentials would generate a higher concentration or wider variety of oxidising agents to degrade the organic material [31]. It is possible that, at such a high electrode potential, other secondary reactions, such as oxygen evolution might occur, resulting in a low concentration of the radical hydroxyl ions formed by the photocatalytic process and the removal of the MO being less efficient. In addition, the drop in efficiency at a potential of 1.75 V *vs*. Ag/AgCl could be due to the structure and the electrical conductivity of the titanium dioxide nanotubes beginning to degrade, as reported by Roy et al., [33].

Experimental results shown in Figures 5 and 6 can be modelled by a pseudo-first order batch kinetics approach. In photoelectrocatalytic processes, this type of model could be explained in terms of a mass transfer control of the rate (Eq. 1) and/or in terms of a pseudo steady state concentration of oxidants produced in the bulk (Eq. 2), for direct or mediated oxidation processes, respectively. This approach has been proposed and applied successfully by Polcaro et al., [37] in previous oxidation studies of pollutants.

$$r = k_m \times A \times [\text{Pollutant}] = K \times [\text{Pollutant}] \quad (1)$$

$$r = k' \times [\text{Oxidant agents}] \times [\text{Pollutant}] = K \times [\text{Pollutant}] \quad (2)$$

where r is the reaction rate, k_m is the mass transfer coefficient and K is the apparent first order rate constant. Figure 7 shows the first order rate constants calculated taking into account this pseudo-first order kinetics approach.

The rate constant increases at higher flow rate, achieving its highest value at 100 L h^{-1} when the applied potential was 1.5 V *vs.* Ag/AgCl. This is consistent with the results shown in Figure 5, and indicates mass transport control. On the other hand, an increase of the applied potential entails a decrease of the oxidation rate, with a kinetic constant even lower than the calculated for the experiment at a potential of 1.5 V *vs.* Ag/AgCl and a volumetric flow rate of 60 L h^{-1}. This can be explained in terms of a oxidation of the structure and lowering of the conductivity of the titanium dioxide nanotubes at 1.75 V [33]. The results indicate that an applied potential of 1.5 V and a flow rate of 100 L h^{-1} (23.0 cm s^{-1}) seem to be appropriate values of these parameters for an efficient oxidation of methyl orange by photoelectrocatalytic oxidation in this study. The values of rate constant are similar to those obtained by Martín de Vidales et al., [12, 38] for the removal of persistent organic pollutants in wastewaters by conductive diamond electrochemical oxidation and electro-irradiated processes (0.005-0.010 min^{-1}).

4. Conclusions

1. The synthesis of a TiO_2 nanotubular array, by anodising in a NH_4F electrolyte, allows efficient oxidation of MO (as a model dye pollutant), from synthetic wastewater by photoelectrocatalytic oxidation.

2. An increase in the flow rate improves the efficiency of the process which suggests that, at the electrode potential used, the process is mass transport controlled.

3. When the electrode potential increases the process efficiency does not improve might be because the oxidant agents generated are not sufficient to degrade the organic molecule or the structure and conductivity of titanium dioxide nanotubes might be degraded at the high positive potential of 1.75 V *vs.* Ag/AgCl,

4. The processes can be fitted to pseudo-first order kinetics and the apparent rate constants are calculated, indicating that the oxidation rate increases with the flow rate and decreases at more positive applied potentials.

Acknowledgements

The authors acknowledge the funding support from the National Spanish Ministry of Economy and Competition (Project CTM2010-18833/TECNO) and the *Formación de Profesorado Universitario* grant (Spanish Government) and the CYTEMA-Puente grant (University of Castilla-La Mancha) for María José Martín de Vidales. The authors are also grateful to Sao Paulo Research foundation (FAPESP) project 2011/51226-3, Sao Paulo Federal University (UNIFESP) from the Brazilian Government and the University of Southampton for the Financial Support.

References

[1] Y. Wong, J. Yu, *Water Res.* 1999, *33(16)*, 3512-3520. DOI:10.1016/S0043-1354(99)00066-4

[2] N. Mohan, N. Balasubramanian, V. Subramanian, *Chem. Eng. Technol.* 2001, *24(7)*, 749-753. DOI: 10.1002/1521-4125(200107)

[3] P. Cañizares, F. Martínez, C. Jiménez, J. Lobato, M.A. Rodrigo, *Environ. Sci. Technol.* 2006, *40(20)*, 6418-6424. DOI: 10.1021/es0608390

[4] M. Zarezadeh-Mehrizi, A. Badiei, A.R. Mehrabadi, *J. Mol. Liq.* 2013, *180 (April)*, 95-100. DOI:10.1016/j.molliq.2013.01.007

[5] Z. Yang, H. Yang, Z. Jiang, T. Cai, H. Li, H. Li, A. Li, R. Cheng, *J. Hazard. Mater.* 2013, *254-255(June)*, 36-45. DOI:10.1016/j.jhazmat.2013.03.053

[6] F. Deniz, *Mater. Sci. Eng., C.* 2013, *33(5)*, 2821–2826. DOI:10.1016/j.msec.2013.03.009

[7] I. Sirés, P.L. Cabot, F. Centellas, J.A. Garrido, R.M. Rodríguez, C. Arias, E. Brillas, *Electrochim. Acta* 2006, *52(1)*, 75-85. DOI: 10.1016/j.electacta.2006.03.075

[8] E. Guinea, C. Arias, P.L. Cabot, J.A. Garrido, R.M. Rodríguez, F. Centellas, E. Brillas, *Water Res.* 2008, *42(1-2)*, 499-511. DOI:10.1016/j.watres.2007.07.046

[9] M. Panizza, A. Kapalka, Ch. Comninellis, *Electrochim Acta* 2008, *53(5)*, 2289-2295. doi:10.1016/j.electacta.2007.09.044

[10] P. Cañizares, R. Paz, C. Sáez, M.A. Rodrigo, *Electrochim. Acta* 2008, *53(5)*, 2144-2153. DOI:10.1016/j.electacta.2007.09.022

[11] M. Mascia, A. Vacca, A.M. Polcaro, S. Palmas, J. Rodriguez-Ruiz, A. Da Pozzo, *J. Hazard. Mater.* 2010, *174(1-3)*, 314–322. DOI:10.1016/j.jhazmat.2009.09.053

[12] M.J. Martín de Vidales, C. Sáez, P Cañizares, M.A. Rodrigo, *J. Chem. Technol. Biotechnol.* 2012, *87(2)*, 225-231. DOI: 10.1002/jctb.2701

[13] M.J. Martín de Vidales, C. Sáez, P. Cañizares, M.A. Rodrigo, *J. Chem. Technol. Biotechnol.,* 2012, *87(8)*, 1173-1178. DOI: 10.1002/jctb.3742

[14] M.J. Martín de Vidales, C. Sáez, P. Cañizares, M.A. Rodrigo, *J. Chem. Technol. Biotechnol.* 2012, *87(10)*, 1441-1449. DOI: 10.1002/jctb.3766

[15] S. Cotillas, J. Llanos, P. Cañizares, S. Mateo, M.A. Rodrigo, *Water Res.* 2013, 47(5), 1741-1750. DOI:10.1016/j.watres.2012.12.029

[16] M.J. Martín de Vidales, C. Sáez, P. Cañizares, M.A. Rodrigo, *J. Chem. Technol. Biotechnol.* 2013, *88(5)*, 823-828. DOI: 10.1002/jctb.3907

[17] M. Ureña de Vivanco, M. Rajab, C. Heim, T. Letzel, B. Helmreich, *Chem. Eng. Technol.* 2013, *36(2)*, 355-361. DOI: 10.1002/ceat.201200478

[18] E. Brillas, C.A. Martínez-Huitle, *Appl. Catal., B* 2015, *166-167(May)*, 603-643. DOI:10.1016/j.apcatb.2014.11.016

[19] J.C. Cardoso, T.M. Lizier, M.V.B. Zanoni, *Appl. Catal., B.* 2010, *99(1-2)*, 96–102. DOI:10.1016/j.apcatb.2010.06.005

[20] P. Bansal, D. Sud, *J. Mol. Catal. A: Chem.* 2013, *374-375(August)*, 66-72. DOI:10.1016/j.molcata.2013.03.018

[21] G.G. Bessegato, J.C. Cardoso, M.V.B. Zanoni, *Catal. Today* 2015, *240(February)*, 100-106. DOI:10.1016/j.cattod.2014.03.073

[22] H. Wu, Z. Zhang, *J. Solid State Chem.* 2011, *184(12)*, 3202–3207. DOI:10.1016/j.jssc.2011.10.012

[23] Y. Wang, J. Lin, R. Zong, J. He, Y. Zhu, *J. Mol. Catal. A: Chem.* 2011, *349(1-2)*, 13-19. DOI:10.1016/j.molcata.2011.08.020

[24] G.K. Mor, K. Shankar M. Paulose, O.K. Varghese, C.A. Grimes, *Nano Lett.* 2005, *5(1)*, 191-195. DOI: 10.1021/nl048301k

[25] Z.B. Xie, D.J. Blackwood, *Electrochim. Acta* 2010, *56(2)*, 905–912. DOI:10.1016/j.electacta.2010.10.004

[26] J.N. Nian, H. Teng, *J. Phys. Chem. B* 2006, *110(9)*, 4193-4198. DOI: 10.1021/jp0567321

[27] J. Yu, H. Yu, B. Cheng, C. Trapails, *J. Mol. Catal. A: Chem.* 2006, *249(1-2)*, 135-142. DOI:10.1016/j.molcata.2006.01.003

[28] S. Zhang, W. Li, Z. Jin, J. Yang, J. Zhang, Z. Du, Z. Zhang, *J. Solid State Chem.* 2004, *177(4.5)*, 1365-1371. DOI:10.1016/j.jssc.2003.11.027

[29] O.K. Varghese, D. Gong, M. Paulose, C.A. Grimes, E.C. Dickey, *J. Mater. Res*. 2003, *18(1)*, 156-165. DOI: 10.1557/JMR.2003.0022

[30] R. Chaiyont, C. Badoe, C. Ponce de León, J.L. Nava, F.J. Recio, I. Sirés, P. Herrasti, F.C. Walsh, *Chem. Eng. Technol*. 2013, *36(1)*, 123-129. DOI: 10.1002/ceat.201200231

[31] H. Ma, B. Wang, X. Luo, *J. Hazard. Mater* 2007, *149(2)*, 492-498. DOI:10.1016/j.jhazmat.2007.04.020

[32] G. Foti, D. Gandini, C. Comninellis. *Curr. Top. Electrochem.* 1997, *5*, 71.

[33] P. Roy, S. Berger, P. Schmuki, *Angew. Chem. Int. Ed.* 2011, *50(13)*, 2904–2939. DOI: 10.1002/anie.201001374

[34] Z. Zhou, L. Zhu, J. Li, H. Tang, *J. Appl. Electrochem.* 2009, *39(10)*, 1745-1753. DOI10.1007/s10800-009-9869-3

[35] Q. Zheng, C. Lee, *Electrochim. Acta* 2014, *115(January)*, 140-145. DOI:10.1016/j.electacta.2013.10.148

[36] F. Walsh, *AIChE Journal* 1996, *42(4)*, 1195-1197. DOI: 10.1002/aic.690420437

[37] A.M. Polcaro, S. Palmas, F. Renoldi, M. Mascia, *J. Appl. Electrochem*. 1999, *29(2)*, 147-151. DOI: 10.1023/A:1003411906212

[38] M.J. Martín de Vidales, S. Barba, C. Sáez, P. Cañizares, M.A. Rodrigo, *Electrochim. Acta* 2014, *140(September)*, 20-26. DOI:10.1016/j.electacta.2014.02.118

Figure captions

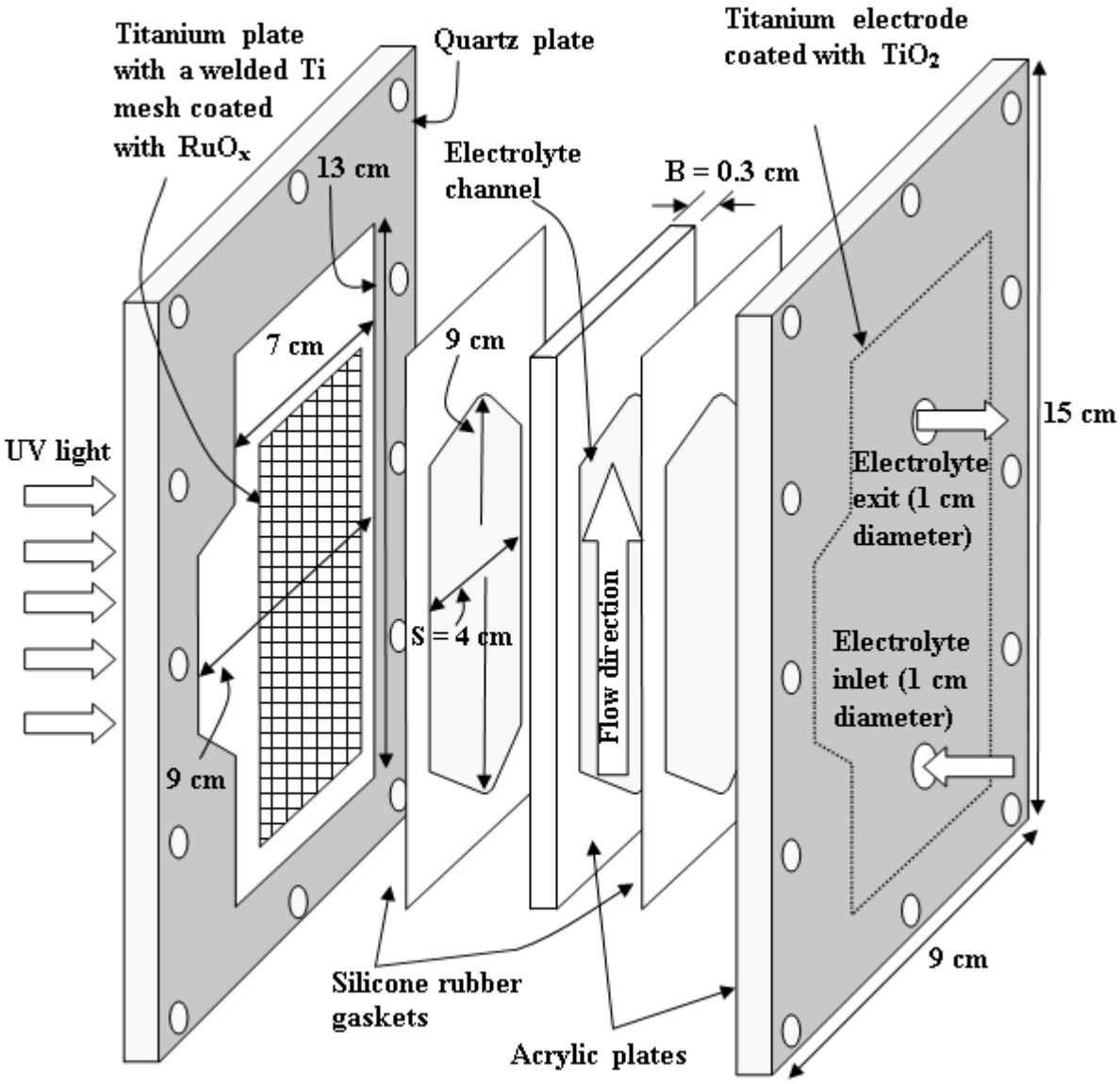

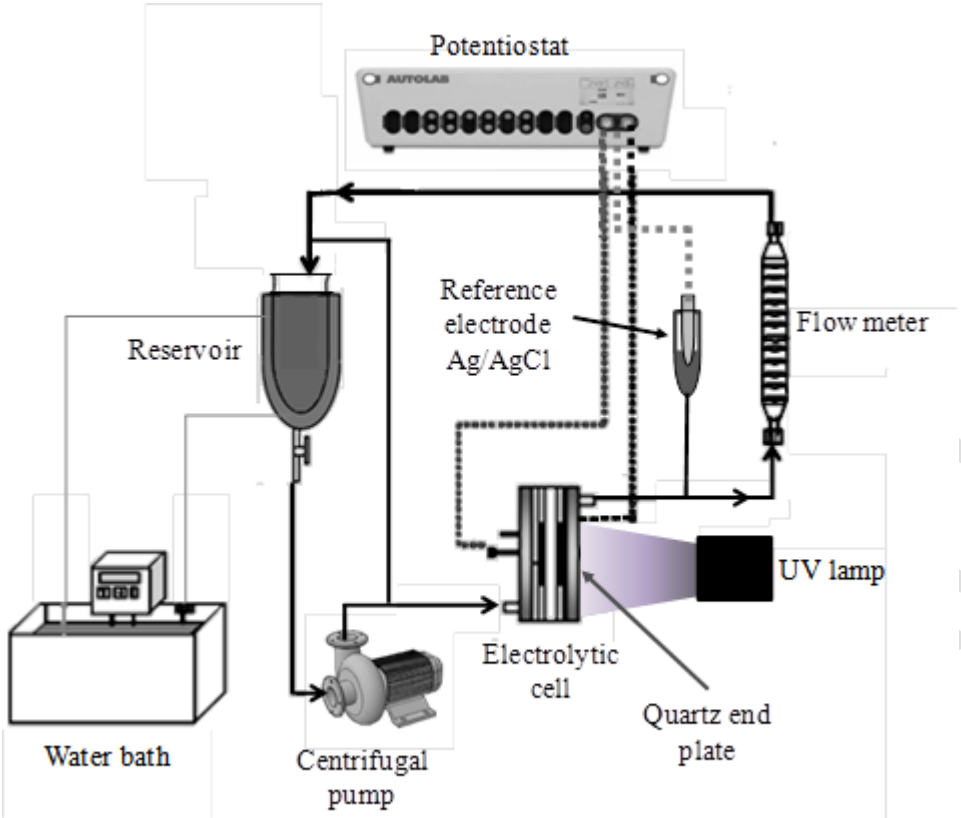

Figure 1 a) Expanded view of the electrochemical cell and b) the electrolytic circuit.

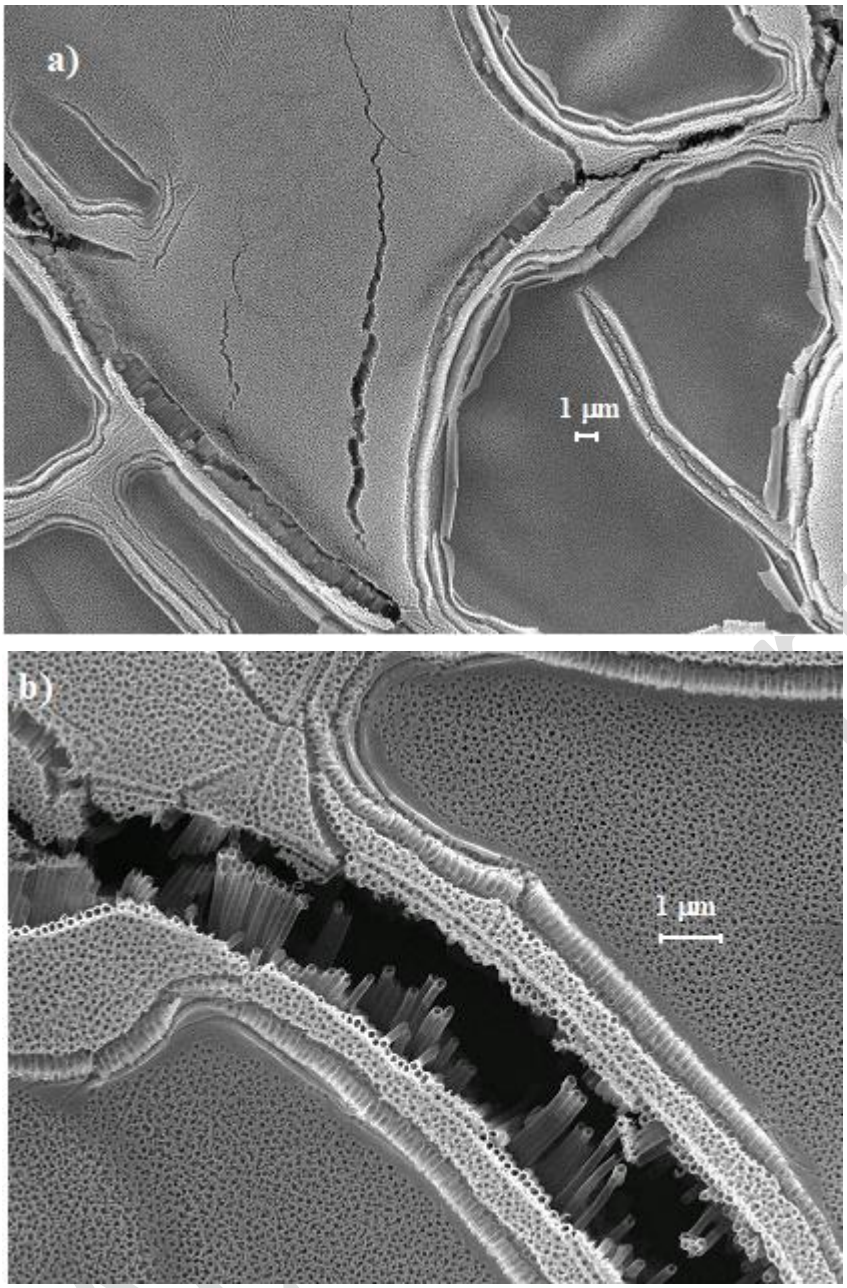

Figure 2 SEM images of the surface of anodized Ti plate electrode in 0.1 mol L^{-1} NH_4F, 2 % vol. water in ethylene glycol, at a cell potential of 40 V followed by heat treatment; a) formation of TiO_2 at different levels on the Ti plate, b) closer view of the TiO_2 nanotubes.

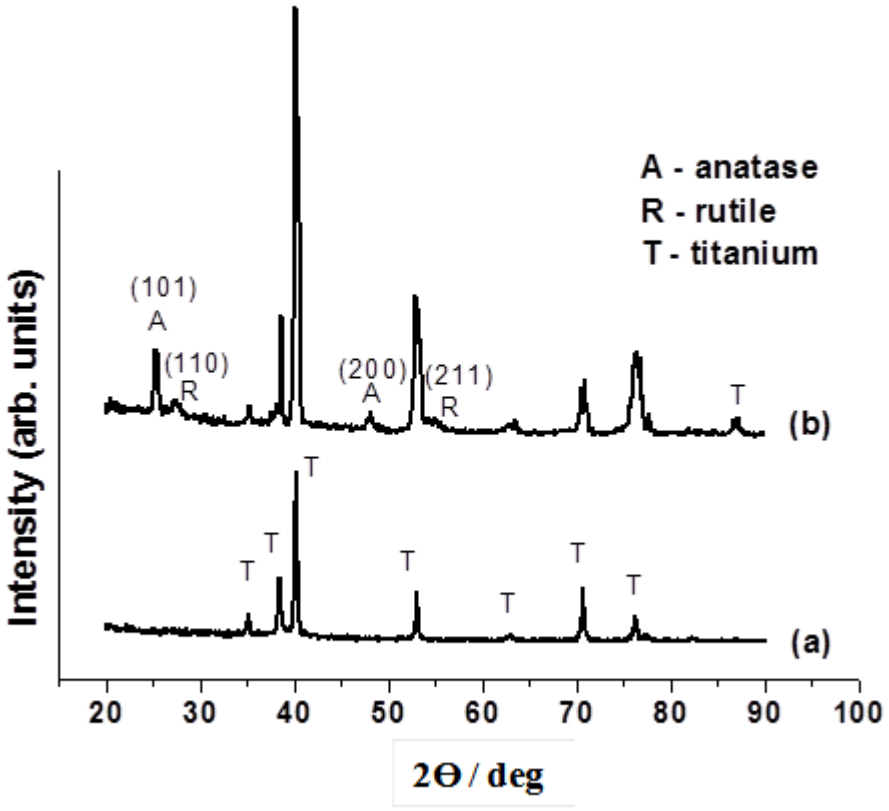

Figure 3 X-ray diffractograms of the nanotube samples a) before and b) after annealing at a temperature of 450 °C in air for 150 minutes. A, R, and T represent anatase, rutile, and titanium, respectively.

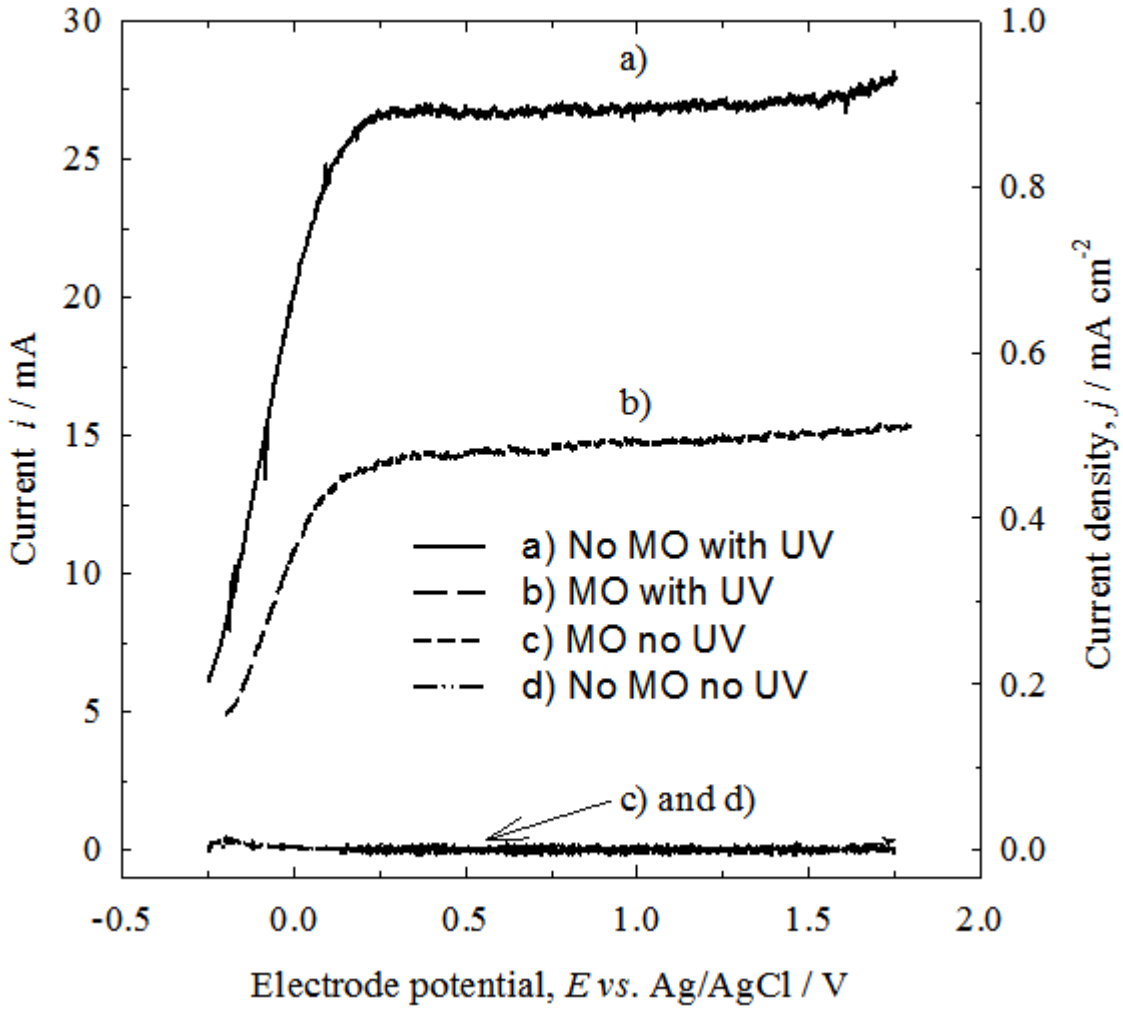

Figure 4 Voltammetry study of the influence of the pollutant and/or the ultraviolet light irradiation. [MO] = 0.25 mmol L^{-1}. [Na_2SO_4] = 0.1 mol L^{-1}. I_{light} = 20.5 A. Volumetric flow rate = 100 L h^{-1}. Potential sweep rate = 0.01 V s^{-1}.

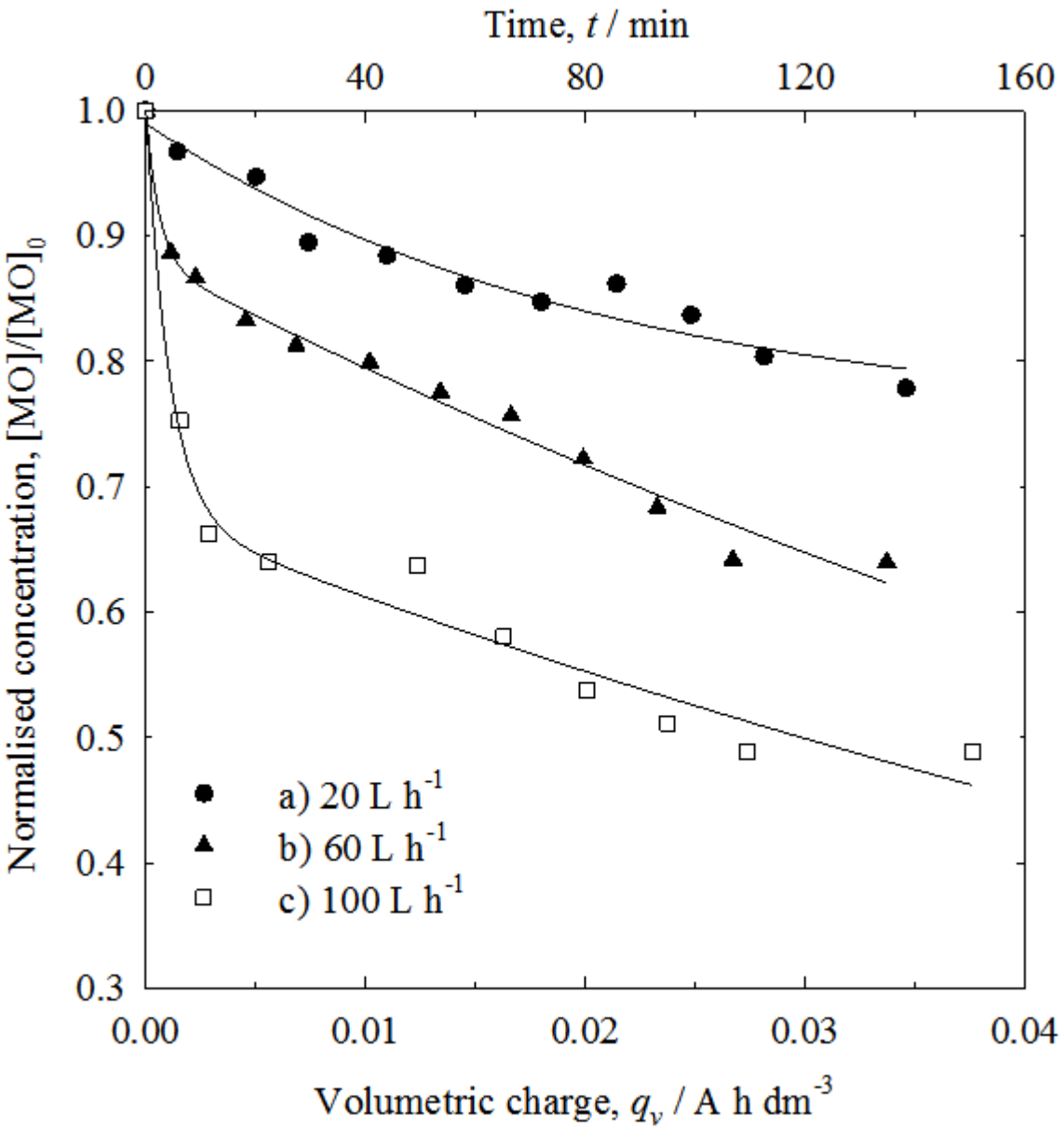

Figure 5 Influence of the flow rate used for the oxidation of methyl orange on the photocatalytic TiO_2 anode. [MO] = 0.25 mmol L^{-1}. [Na_2SO_4] = 0.1 mol L^{-1}. Electrode potential= 1.5 V *vs*. Ag/AgCl. I_{light} = 20.5 A: (*) 20 L h^{-1}, (▲) 60 L h^{-1}, (□) 100 L h^{-1}.

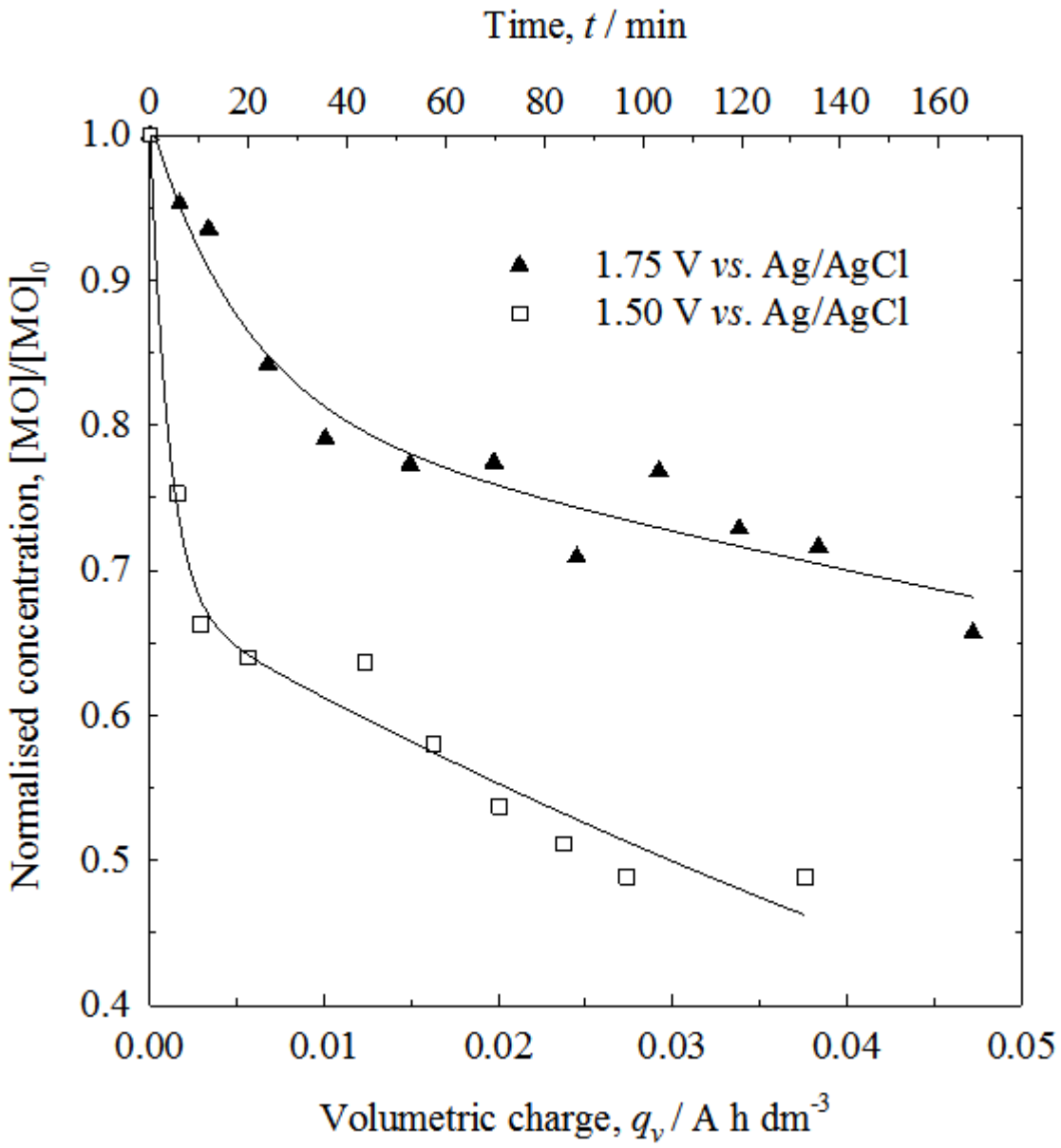

Figure 6 Influence of the applied potential for the oxidation of methyl orange by photoelectrocatalytic oxidation. [MO] = 0.25 mmol L^{-1}. [Na_2SO_4] = 0.1 mol L^{-1}. Flow rate = 100 L h^{-1}. I_{light} = 20.5 A. (▲) 1.75 V *vs*. Ag/AgCl, (□) 1.5 V *vs*. Ag/AgCl.

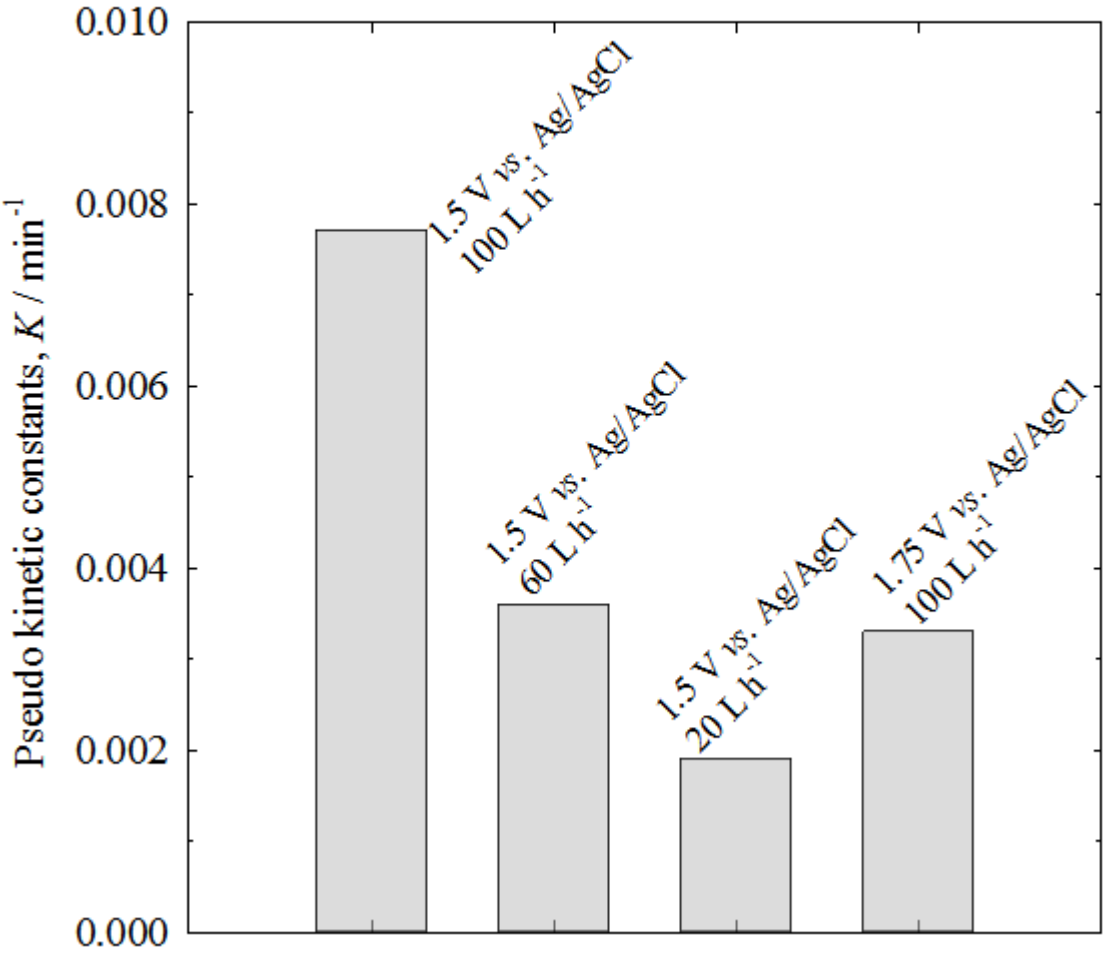

Figure 7 Comparison of the apparent rate constants.

Table of Contents

A photocatalytic anodic oxidation method was used to remove methyl orange from water. The method uses photo catalytic titanium nanotubes that produce hydroxyl radicals able to oxidise the organic molecule. Aqueous solution of methyl orange circulates through a flow cell. The study present the influence of the flow rate, and the applied potential on the removal efficiency.